NEUBOrg: artificially induced pluripotent stem cell-derived brain organoid to model and study genetics of Alzheimer's disease progression.

Sally Esmail
123Genetix
Wayne Danter (wdanter@123genetix.com)
123Genetix

Article

Keywords: Organoid Computer Simulations, Wet Lab Research, Machine Learning, Genetic Risk Factors

Posted Date: December 1st, 2020

DOI: https://doi.org/10.21203/rs.3.rs-111244/v1

Abstract

Alzheimer's disease (AD) is the most common type of neurodegenerative diseases. There are over 44 million people living with the disease worldwide. While there are currently no effective treatments for AD, induced pluripotent stem cell-derived brain organoids have the potential to provide a better understanding of Alzheimer's pathogenesis. Nevertheless, developing brain organoid models is expensive, time consuming and often does not reflect disease progression. Using accurate and inexpensive computer simulations of human brain organoids can overcome the current limitations. Induced whole brain organoids (aiWBO) will greatly expand our ability to model AD and can guide wet lab research. In this study, we have successfully developed and validated artificially induced a whole brain organoid platform (NEUBOrg) using our previously validated machine learning platform, DeepNEU (v6.1). Using NEUBorg platform, we have generated aiWBO simulations of AD and provided a novel approach to test genetic risk factors associated with AD progression and pathogenesis.

Introduction

The modern era of human stem cell research was launched with a publication by Professor Yamanaka's group in 2007 [1]. This landmark paper demonstrated conclusively that human fibroblasts could be transformed, with four transcription factors and optimal conditions, into cells closely resembling human pluripotent stem cells (hPSC). These transformed cells have become widely referred to as induced pluripotent stem cells (iPSC). Since 2007 iPSCs have become a mainstay technology for disease modelling, stem cell therapies, drug discovery and specific cell line differentiation. More recently iPSCs have been used to develop tissue specific spheroids and more complex organoids show some early promise both as research tools and disease specific transplant options [2-4]. An organoid has been defined as an artificially grown mass of cells or tissue that resembles an organ. While still in its infancy, the science of human organoids has been used successfully to develop multiple organoid types including intestine, heart, pancreas, liver, lung and brain to name a few [5].

Cerebral organoids have been produced with some early successes [2, 3]. Cerebral organoids continue to evolve as useful tools for modelling more common chronic and degenerative neurologic diseases like Alzheimer's disease, Parkinson's disease, and rarer neurological disorders like RETT syndrome, Huntington's disease and Zika microcephaly are also amenable to cerebral organoid modelling [6, 7]. In general, any neurologic disease that can be represented in an induced stem cell model can theoretically also be represented in a cerebral organoid. To date, two main approaches have been employed to produce cerebral organoids from human stem cells [8]. These two methods have been labelled as unguided and guided. The unguided approach relies on the tendency of iPSC to develop towards neural precursors if given enough time and an optimal cellular environment. The guided method uses sequential combinations of small molecules and modified media to generate cerebral organoids. Both methods produce organoids that take many months to mature, result in recognizable and semi-organized cerebral tissue with similar limitations. Growing cerebral organoids in vitro has been challenging in a number of

important ways. For example, modelling cerebral vasculature and a functional blood brain barrier remain problematic [4, 8-11]. In addition, the in vitro organoids lack a blood supply and this important deficit results in a variable amount of central necrosis as the organoids outgrow the ability of diffusion to deliver oxygen, nutrients and remove toxic waste by products [12].

More complex whole brain organoids represent a logical advancement of cerebral organoids. This technology attempts to reproduce forebrain, midbrain and hindbrain structures with rostral-caudal as well as ventral-dorsal organization. The development of whole brain organoids has been advanced by combining regionally specific organoids in vitro like cerebral, cerebellar, retinal organoids and directing the development of functional vascular elements [13]. Rotating bioreactors with complex media have provided additional improvement in evolving whole brain organoids [14]. Overall, this process is technologically demanding and requires considerable time and expense to achieve modest results. A recent study has concluded that at present, whole brain organoids do not faithfully reproduce all elements of the human brain [15]. This is particularly true regarding the internal architecture and neural connections. One suggested explanation for the observed differences could be the significant and multiple stresses that occur during the growth and development of iPSC and avascular organoids over protracted periods of time. This suggestion is supported by the observation that transplanted brain organoids tend to become more organized and representative of the native neural tissue [15].

We believe that the future for whole brain organoid research including novel therapeutic possibilities is quite promising and to date remarkable progress has been achieved [5]. Given the considerable cost and limitations of current *in vitro* derived whole brain organoids we also believe that validated, easily customizable and relatively inexpensive computer simulations of artificially induced whole brain organoids (aiWBO) could represent an important step forward. Such a technology could be an important tool for simulating many neurological diseases and lead to important new therapeutic insights to guide wet lab research in a timely and cost-effective manner.

Modeling Alzheimer disease using iPSC-derived brain cells

Alzheimer's disease (AD) is the most common chronic neurodegenerative disease characterized by progressive loss of cognition and disruption of basic functions, such as swallowing, walking, attention, and memory [16]. AD is the sixth leading cause of death in the United States and the fifth leading cause of death among seniors [17]. Increasing evidence has suggested that loss or dysfunction of different brain cell types likely contribute to AD progression [18]. Thus, modeling these cells and examining their interactions will shed mechanistic insights into AD pathogenesis. Accordingly, significant efforts have been put to building models that incorporate multiple iPSC-derived brain cell types. However, the ability to obtain iPSC-derived brain cells that mimic human brain remains a significant challenge. Validated whole brain organoid simulations could represent an important tool for enabling neurodegenerative disease modelling, biomarker identification and drug discovery.

The main purpose of this project was to extend our previous DeepNEU research [19-21] by developing and validating aiWBO using the latest validated version of the DeepNEU (v6.1) machine learning platform. In this study, the DeepNEU platform was used to generate aiWBO simulations of AD. To our knowledge this is the first time that a simulation of a Whole Brain Organoid has been attempted. These aiWBO simulations have been named NEUBOrg.

Methods

The DeepNEU stem cell simulation platform is a literature validated hybrid deep-machine learning system with elements of fully connected recurrent neural networks (RNN), cognitive maps (CM), support vector machines (SVM) and evolutionary systems (GA). The detailed methodology for simulation development and validation plus the description of the evolving DeepNEU database used in these experiments has been described previously in detail [19-21].

The current DeepNEU database (v6.1) contains the information found in the previous version (v5.0) plus an important information upgrade in the form of new genotypic concepts, phenotypic concepts and relationships. The majority of these new concepts and relationships were used to generate signatures for identifying specific cell types, brain regions, cortical layers, the blood brain barrier and provide evidence of a rudimentary circulation. For example, the previous DeepNEU database (v5.0) contained 4206 gene/proteins or phenotypic concepts and 37223 nonzero relationships while the current version (6.1) contains 4516 gene/proteins or phenotypic concepts and 41493 nonzero relationships. This represents more than 4700 new relationships specifically relevant to developing whole brain organoids. Each gene/protein and phenotypic concept in DeepNEU (v6.1) has on average more than 9 gene/protein or phenotypic inputs and outputs.

The DeepNEU simulations

The NEUBOrg Whole Brain Organoid (aiWBO) simulations

The main purpose of this project was to extend our previous DeepNEU research by developing and validating a whole brain organoid simulation (aiWBO) using the latest version of the DeepNEU (v6.1) machine learning platform. To accomplish this, we used an approach similar to that described by Yamanaka 2007 [1] to transform human fibroblasts into induced pluripotent stems cells (iPSC). Several important modifications to the original 2007 protocol were required to promote differentiation from aiPSC to aiWBO. The modified protocol began with the activation of four transcription factors OCT4, cMYC, KLF4 and SOX2. In addition, we used a simulated B27 neural media with supplementary Zinc and Ascorbic acid in the presence of Doxycycline and normal levels of ambient Oxygen (21%). For all simulations age was fixed at 65 years of age. The aiPSC to aiWBO transformation using the above cocktail was carried out in a simulated rotating bioreactor which has been shown to improve the production of WBO from iPSCs. All aiWBO simulation experiments were carried out in triplicate. The complete cocktail is summarized below in Table 1.

Table 1: Unguided aiPSC to aiWBO simulation cocktail

Cocktail	Components (simulated)
Yamanaka (2007) transcription factors	OCT4, cMYC, KLF4 and SOX2 turned ON
B27 neural media	Biotin, Amino Acids, Ascorbate, Catalase, Cortisol, FGF2/bFGF, Glutathione, Albumin, Insulin, SOD1(Cu/Zn), MnSOD/SOD2, Progesterone, Retinol/Vitamin A, Thyroid Hormones (T3/T4), Transferrin, VitE/Tocopherol, L-Carnitine locked ON
Supplements	Zinc and Doxycycline locked ON
Rotating bioreactor (optimized)	B27 media + [CO2] =5%, [O2] =21%, Glucose, Temperature=37 degrees C locked ON and High shear forces locked OFF
Age	65 years of age locked ON

The aiWBO were designed to simulate the (i) diverse neural cell types, (ii) rostral caudal brain regions, (iii) ventral dorsal regions where possible and the (iv) six horizontal layers of the cerebral cortex and (v) the four layers of the cerebellar cortex. The spinal cord was not simulated in the current project. The main cell types included are neurons, astrocytes, oligodendrocytes and microglial cells. Additional cell types include endothelial cells and pericytes which are important components of the blood brain barrier (BBB). The rostral caudal regions simulated include forebrain, midbrain and hindbrain. The ventral dorsal regions include ventral forebrain etc. The horizontal layers of the cerebral cortex arranged from outer to inner include Layers 1-6 and the 4 main layers of the cerebellar cortex from outer to inner are also simulated. NEUBOrg platform, aiWBO simulations, was built based on the following comprehensive literature to provide genotypic and phenotypic markers for identifying cell types, brain regions and cortical layers [2-8, 11-15, 22-36]. A compilation of relevant markers is presented in Tables S1, S2, S3, S4, and S5.

The NEUBOrg Whole Brain Organoid simulations applied to Alzheimer's Disease

Once validated, the unguided aiWBO were used to simulate a whole brain organoid affected by Alzheimer's disease. To accomplish the disease simulations (aiWBO-APOE4) two concepts were modified. First, APOE4 was locked ON to simulate an APOE4 duplication/GOF mutation. To simulate an important inhibitory effect of an APOE4 mutation, beta amyloid clearance was locked OFF. The cocktail and process were otherwise identical to that outlined above for the developing the wild type aiWBO simulations. All aiWBO-APOE4 (AD) simulation experiments were carried out in triplicate.

A detailed literature review of genotypic and phenotypic features was used to develop a profile of Alzheimer's Disease that we used to evaluate the performance of the AD simulations compared to the aiWBO [22, 27, 29, 37-43]. Negative inputs inhibit the feature while positive inputs promote the feature. A

compilation of the large number and status of inputs that constitute the AD feature profile is presented in Table 2 below.

Table 2: Alzheimer's Disease Feature Profile

Alzheimer's Disease (AD) Features (N=10)	Genotypic/Phenotypic Feature Inputs
Amyloid Beta Plaques	N=9, 3 negatives + 6 positives
Amyloid Beta Protein (42/40) Clearance	N=51, 23 negatives + 28 positives
Amyloid Beta Protein (Ab1-42/Ab1-40)	N=47, 24 negatives + 23 positives
Amyloid-Beta-Oligomers/aggregation	N=45, 23 negatives + 22 positives
ApoE4(>ApoE3)	N=17, 8 negatives + 9 positives
APP/Amyloid precursor protein	N=50, 24 negatives + 26 positives
NFTs/Neurofibrillary Tangles	N=10, 4 negatives + 6 positives
Tau Proteins/MAPT	N=27, 16 negatives + 11 positives
Tau Protein Phosphorylated	N=52, 25 negatives + 27 positives
Tau Protein Aggregation	N=10, 3 negatives + 7 positives

DeepNEU platform statistical analysis

Consistent with previously projects, the statistical analysis of all aiWBO and aiWBO-APOE4 predictions vs the published and previously unseen wet lab data used the unbiased binomial test. This test provides an exact probability, can compensate for prediction bias, and is ideal for determining the statistical significance of experimental deviations from an actual distribution of observations that fall into two outcome categories (e.g. agree vs disagree). A p value <0.05 is considered significant and is interpreted to indicate that the observed relationship between aiWBO and aiWBO-APOE4 predictions and actual outcomes is unlikely to have occurred by chance alone. For other between group (e.g. aiWBO vs aiWBO-APOE4) comparisons, the Mann-Whitney u test of significance was used [44]. This nonparametric test was chosen because some of the data was not normally distributed

Results

The DeepNEU platform specification

The current DeepNEU database (v6.1) contains 4516 gene/protein or phenotypic concepts and 41493 nonzero relationships resulting in a large amount of information flowing into and out of each node in the fully connected recurrent network. On average, each node in the network initially has >9 inputs and >9

outputs. An updated analysis of all positive and negative network connections revealed a bias toward positive outputs. The pretest probability of a positive outcome prediction is 0.656 and the pretest probability of a negative prediction is therefore 0.344. This system bias was used when applying the binomial test to all simulation outcomes.

The aiWBO Wild Type Simulations

The unsupervised whole brain organoid (aiWBO) simulations converged quickly (45 iterations) to a new system wide steady state without evidence of overtraining after 1000 iterations.

Neural Cell Types

The aiWBO correctly predicted the expression of all 6 neural cell types commonly found in human brain organoids. The probability that all (N = 6) cell type outcomes were predicted by chance alone using the binomial test is 0.08. These results are summarized in Figure 1A.

Rostral-Caudal Brain Regions

The aiWBO correctly predicted the expression of all 3 regions commonly found in human brain organoids. These regions are Forebrain, Midbrain and Hindbrain. The spinal cord was not simulated in the current version. The probability that the expression of all (N = 3) regions were predicted by chance alone using the binomial test is 0.282. These results are summarized in Figure 1B.

Ventral-Dorsal Brain Regions

The aiWBO correctly predicted the expression of all 7 ventral (anterior)-dorsal (posterior) regions commonly found in human brain organoids. The probability that the expression of all (N = 7) regions were predicted by chance alone using the binomial test is 0.052. These results are summarized in Figure 1C.

Acid-Base status of the organoid

The aiWBO predicted the expression of all 7 concepts representative of a mixed (compensated) metabolic-alkalosis and respiratory acidosis in human brain organoids. The probability that the expression of all (N = 7) concepts associated with the expression of a compensated metabolic-alkalosis and respiratory acidosis were predicted by chance alone using the binomial test is 0.052. These results are summarized in Figure 1D.

Cerebral Cortical Layers

The aiWBO correctly predicted the expression of all 6 cerebral cortical layers commonly found in human brain organoids. The probability that the expression of all (N = 6) cerebral cortical layers were predicted by chance alone using the binomial test is 0.08. These results are summarized in Figure 2A.

Cerebellar Cortical Layers

The aiWBO correctly predicted the expression of all 4 cerebellar layers cortical commonly found in human brain organoids. The probability that the expression of all (N = 4) cerebral cortical layers were predicted by chance alone using the binomial test is 0.185. These results are summarized in Figure 2B.

Microcirculation

The aiWBO correctly predicted the expression of all 7 concepts representative of a microcirculation in human brain organoids. The probability that the expression of all (N = 7) concepts associated with the expression of a microcirculation were predicted by chance alone using the binomial test is 0.052. These results are summarized in Figure 2C.

Blood Brain Barrier (BBB)

The aiWBO correctly predicted the expression of all 6 concepts representative of a BBB in human brain organoids. The probability that the expression of all (N = 6) concepts associated with the expression of a BBB were predicted by chance alone using the binomial test is 0.185. These results are summarized in Figure 2D.

Summary Results for aiWBO simulations

Taken together the aiWBO correctly predicted the expression of 39 elements consistent with a pattern seen in a whole brain organoid and 7 elements consistent with the presence of a compensated metabolic-alkalosis and respiratory acidosis. The probability that the expression of all (N = 46) concepts were predicted by chance alone using the binomial test is <0.00000001.

The aiWBO-APOE4 Alzheimer's Disease (AD) Simulations

The unsupervised whole brain organoid (aiWBO-APOE4) AD simulations converged quickly (42 iterations) to a new system wide steady state without evidence of overtraining after 1000 iterations

Neural Cell Types

The aiWBO-APOE4 (AD) simulations correctly predicted the expression of all 6 neural cell types commonly found in human brain organoids. The probability that all (N = 6) cell type outcomes were predicted by chance alone using the binomial test is 0.08. A statistical analysis using the Mann-Whitney u test indicated that there were significant decreases in the expression of astrocytes and oligodendrocytes with the AD simulations. All other cell types including neurons were not significantly different between aiWBO and AD simulations. These results are summarized in Figure 3A.

While the major cell target of advanced AD is neurons, deleterious effects on synapses are among the earliest pathologic changes. When we examined the impact of increased APOE4 on the AD simulations

using a 7-element, literature validated profile, the effects were largely consistent with significant decline in synaptogenesis and synaptic function. These results are summarized in Table 6S.

Rostral-Caudal Brain Regions

The aiWBO-APOE4 (AD) simulations correctly predicted the expression of all 3 regions commonly found in human brain organoids. These regions are Forebrain, Midbrain and Hindbrain. The spinal cord was not simulated in the current version. The probability that the expression of all (N = 3) regions were predicted by chance alone using the binomial test is 0.282. A statistical analysis using the Mann-Whitney u test indicated that there was a small but significant ($p<0.05$) decrease in the expression of the Forebrain and small but significant increase in the Midbrain while the Hindbrain was unchanged in the AD simulations. These results are summarized in Figure 3B.

Ventral-Dorsal Brain Regions

The aiWBO-APOE4 (AD) simulations correctly predicted the expression of all 7 ventral (anterior)-dorsal (posterior) representative regions commonly found in human brain organoids. The probability that the expression of all (N = 7) regions were predicted by chance alone using the binomial test is 0.052. A statistical analysis using the Mann-Whitney u test indicated that there were no significant differences ($p>0.05$) in the expression of all Ventral-Dorsal brain regions in the aiWBO and AD simulations. These results are summarized in Figure 3C.

Cerebral Cortical Layers

The aiWBO-APOE4 (AD) simulations correctly predicted the expression of all 6 cerebral cortical layers commonly found in human brain organoids. The probability that the expression of all (N = 6) cerebral cortical layers were predicted by chance alone using the binomial test is 0.08. A statistical analysis using the Mann-Whitney u test indicated that there was a significant decrease ($p<0.01$) in the expression of the Layers 2-5 with a very small but still significant decrease ($p<0.05$) Layer 6. Layer 1 was unchanged in the AD simulations. Overall, there was also a significant decrease in cerebral cortical mass in AD simulations. These results are summarized in Figure 3D.

Cerebellar Cortical Layers

The aiWBO-APOE4 (AD) simulations correctly predicted the expression of all 4 cerebellar cortical layers commonly found in human brain organoids. The probability that the expression of all (N = 4) cerebral cortical layers were predicted by chance alone using the binomial test is 0.185. A statistical analysis using the Mann-Whitney u test indicated that there were no significant differences ($p>0.05$) between expression of all cerebellar cortical layers in the aiWBO and AD simulations. These results are summarized in Figure 3E.

Microcirculation

The aiWBO-APOE4 (AD) simulations correctly predicted the expression of all 7 concepts representative of a microcirculation in human brain organoids. The probability that the expression of all (N = 7) concepts associated with the expression of a microcirculation were predicted by chance alone using the binomial test is 0.052. A statistical analysis using the Mann-Whitney u test indicated that there were significant decreases ($p<0.05$) in the endothelial-arterial, venous and lymphatic components of the Microcirculation in the AD simulations. In addition, the intracellular O2 concentration is significantly decreased ($p<0.05$) in the AD simulations consistent with a degree of microcirculation impairment. These results are summarized in Figure4A.

Blood Brain Barrier (BBB)

The aiWBO-APOE4 (AD) correctly predicted the expression of all 6 concepts representative of a BBB in human brain organoids. The probability that the expression of all (N = 6) concepts associated with the expression of a BBB were predicted by chance alone using the binomial test is 0.185. A statistical analysis using the Mann-Whitney u test indicated that there were significant decreases in the astrocyte ($p<0.05$) and pericyte ($p<0.01$) components of the BBB. In addition, the function of the BBB was significantly decreased ($p<0.01$) in the AD simulations while the expression of the BBB itself was not different. These results are summarized in Figure 4B.

Acid-Base status of the organoid

The aiWBO-APOE4 (AD) simulations predicted the expression of all 7 concepts representative of a mixed (compensated) metabolic-alkalosis and respiratory acidosis in human brain organoids. The probability that the expression of all (N = 7) concepts associated with the expression of a compensated metabolic-alkalosis and respiratory acidosis were predicted by chance alone using the binomial test is 0.052. A statistical analysis using the Mann-Whitney u test indicated that there were significant changes ($p<0.05$) in all components of the AD simulations compared with aiWBO. Most notable there is a significant increase in intracellular H+ concentration. Taken together these data suggest a somewhat less well compensated mixed metabolic alkalosis- respiratory acidosis in the AD simulations. The persistent high CO2 concentration is also consistent with the increased CO2 concentration (5%) that is part of the cocktail used in generating aiWBO and AD simulations. These results are summarized in Figure 4C.

The aiWBO-APOE4 Alzheimer's Disease (AD) simulations

The aiWBO-APOE4 simulations predicted the expression of all 10 concepts, representative of the Alzheimer's Disease (AD) disease profile, in a simulated human brain organoid. The probability that the expression of all (N = 10) AD concepts were predicted by chance alone using the binomial test is 0.015. A statistical analysis using the Mann-Whitney u test indicated that there were significant changes ($p<0.001$) in all components of the simulated AD disease profile, except for the expression of amyloid precursor protein (APP) when compared with aiWBO. These results are summarized in Figure 4D.

Summary of AD simulations

While the AD simulations produced some significant variability when compared with the aiWBO simulation outputs, the AD simulations also correctly predicted the expression of 39 elements consistent with a pattern seen in a whole brain organoid and 7 elements suggesting the expression of a compensated metabolic alkalosis and respiratory acidosis. The probability that the expression of all (N = 46) concepts were predicted by chance alone using the binomial test is <0.00000001.

Discussion

The main purpose of this project was to extend our previous research [19-21] by first developing and then validating a whole brain organoid simulation (aiWBO) using the latest version of the DeepNEU (v6.1) machine learning platform. Our unguided approach toward brain organoid development relied on the natural tendency of iPSC to differentiate towards complex neural outcomes given enough time and optimal physical and environmental conditions. When we evaluated the aiWBO simulations by applying the wet lab, published genotypic and phenotypic features of a whole brain organoid, the results confirm that the simulations performed well in that they reliably reproduced the wet lab profile. The probability that the expression of all (N = 46) features were predicted by chance alone using the binomial test is <0.00000001. The important anatomical and regional aspects of the neonatal brain were all predicted accurately. In addition, the simulations appear to have evolved rudimentary elements of a functioning microcirculation and blood brain barrier. Both elements are limited by the absence of a functioning systemic and cerebral circulation. Importantly, the current level of sophistication of these aiWBO simulations has been achieved without expensive or demanding and time-consuming protocols or the need to grow and then combine individual organoids like cerebral, cerebellar and blood brain barrier into more complex whole brain like structures.

Fortunately, the concepts necessary to evaluate acid base status have always been a core capability of the DeepNEU platform. This allowed us to evaluate the status of these artificial whole brain organoid simulations. Overall, the pattern observed at stabilization was that of a compensated or combined metabolic alkalosis and respiratory acidosis. Importantly, the intracellular H+ ion concentration [iH+] deviation from the arbitrary base line is minimal. The high bicarbonate and CO2 levels round out the mixed profile. Finally, the organoid appears to be adequately oxygenated. At least part of this complex picture is the result of the normal ambient Oxygen level (21%) and increased CO2 (5%) level used in the bioreactor protocol.

Once the aiWBO simulations were validated against the current literature, the DeepNEU platform was be used to generate aiWBO simulations of Alzheimer's disease (AD), an important and increasingly common chronic degenerative neurologic disease. As outlined above in Table 3, a literature derived 10 feature genotypic and phenotypic AD profile was used to evaluate simulation predictions. When we compared the aiWBO simulation outputs with the AD simulations and allowing for disease related effects, both simulations accurately reproduced the feature profile consistent with the pattern seen in a whole brain organoid. To our knowledge this is the first time that a whole brain organoid simulation of Alzheimer's Disease (AD) has been attempted.

Alzheimer's Disease (AD) is known to impact many neural cell types including neurons, oligodendrocytes, astrocytes and microglia (Ref). While more advanced disease largely results in neuronal loss, the current results would suggest that the AD simulations represent an early/milder form of the disease. This conclusion is supported by a number of other factors. Firstly, Age was arbitrarily set at 65 years for the simulations. Based on the available data this age is widely suggested as a reasonable lower limit for late onset AD (LOAD) and above the upper limit for early onset AD (EOAD). In addition, we wanted to explore the impact of an isolated increase in APOE4, so other factors which are known to exacerbate the disease including diabetes, tobacco abuse, obesity, hypertension, dyslipidemia and advanced age were all turned off during simulation generation. Finally, this conclusion is supported by the prediction of a significant decline in new synapses formation and loss of synaptic function in AD simulations. Taken together these results are all consistent with an early or milder form of the disease.

In an attempt to create more anatomically correct whole brain simulations, we evaluated a limited number of (1) Rostral-Caudal features, (2) Ventral-Dorsal features, (3) Cerebral Cortical layers and (4) Cerebellar Cortical layers. In contrast to wet lab whole brain organoids which are variably disorganized, the aiWBO and aiWBO-APOE3 simulations accurately reproduced the basic anatomical organization of human brain regions and cortical layers. We believe that while encouraging, these anatomic results are rudimentary since validated markers for many brain regions are inadequate or unavailable in the current peer reviewed literature. It is certain this will change as new information is published. Importantly, new information can easily be added to the DeepNEU database in real time as it becomes available.

With regard to AD, the current data indicate that the relatively mild disease has small but significant effects on Rostral-Caudal elements but no significant changes in Ventral-Dorsal features. Similarly, there were no significant changes in cerebellar cortical layers. In contrast, there were significant changes in cerebral cortical layers 2-5 and less so in Layer 6. No significant changes were detected in Layer 1. The aiWBO-APOE4 (AD) simulation results are generally similar to published wet lab results and consistent with early but progressive disease. Pathology has previously indicated that Layers 2-4 tend to be affected early while layers 5-6 are affected later and Layer 1 is unaffected.

Most previous attempts to create whole brain organoids have met with limited success with regards to producing a rudimentary microcirculation. Although the organoids are not connected to a functioning cardiovascular system, the presence of a cerebral microcirculation has important implications as a critical element of a functioning blood brain barrier. As summarized in Figure 14, several important elements of a rudimentary microcirculation were present in the wild type aiWBO simulations. Furthermore, it appears that the simulated microcirculation may be impaired in the AD simulations consistent with known effects patients with AD.

Importantly, elements of a rudimentary and functioning blood brain barrier (BBB) were also expressed in the wild type aiWBO simulations. In the AD simulations there were significant decreases in the astrocyte and pericyte components of the BBB. In addition, the function of the BBB was also significantly decreased in the AD simulations. The function of the BBB which was not explored in detail in these initial

experiments, has important nutritional, metabolic and pharmacological implications which will be evaluated in futures experiments with a focus on drug development. The NEUBOrg platform aiWBO simulations should permit the early identification of drugs and other potential therapeutics which either enter or do not enter the central nervous system.

Limitations of the current aiWBO simulations.

In our recent paper, [21], we identified and discussed several limitations of the DeepNEU platform. First, the issue of incomplete data continues to improve on an almost daily basis. Version 5.0 contained 4206 gene/proteins or phenotypic concepts and 37223 nonzero relationships while the current version (6.1) contains 4516 gene/proteins or phenotypic concepts and 41493 nonzero relationships. Overall, the data in v6.1 represents more than 20% of the human genome compared with ~18% in version 5.0. Included in this number is 4270 new relationships specifically relevant to whole brain organoid creation. In addition, each gene/protein and phenotypic concept in DeepNEU v6.1 now has on average >9 gene/protein or phenotypic inputs and outputs. Second, advanced computer modeling systems still require wet lab confirmation, and this continues to be important for DeepNEU v6.1 as well. A major goal of this project was to make these findings regarding the potential research and therapeutic benefits of a validated whole lung simulation of Alzheimer's Disease available to the global research community for wet lab disease modelling, drug discovery and repurposing at the very earliest opportunity. We also plan to continue to develop and validate these important simulations, while focusing on improving the microcirculation and BBB elements of aiWBOs. We are currently seeking development partners with the goal of empowering Cystic Fibrosis research to better understand disease pathology, enable drug discovery and repurposing. We commit to making any additional information available at the earliest opportunity. Third, we have successfully migrated the upgraded DeepNEU platform to the IBM cloud. This emerging technology will permit more rapid organoid simulation development, disease modelling, therapeutic target identification, and drug repurposing for Alzheimer's and other diseases. Finally, our technology continues to evolve from a hybrid deep learning approach towards the Wise Learning (WL) approach described by Groumpos [45].

Conclusions And Future Directions

With the current advances in brain organoid and iPSC-derived brain cells research, the functions of AD risk genes and AD causing mutations in iPSC-derived brain cell types remains largely unexplored. It is important to further our understanding of how such mutations, either alone or in in combination, affect the interactions between the different cell types of the brain is contributing to AD pathogenesis. We conclude that based on data presented here and the continued development of the NEUBOrg platform, our aiWBO simulations will not only contribute to enhancing our knowledge of AD pathogenesis, but also can be expanded to study different neurodegenerative diseases. NEUBOrg holds considerable promise for allowing us to answer previously unanswered questions, and ultimately to identify and implement effective treatments for AD and other diseases that primarily affect the central nervous system.

Declarations

CONFLICTS OF INTEREST

SE and WRD have uncompensated relationship with 123 Genetix medical enterprise, nonetheless the authors declare that they are providing an unbiased scientific article.

References

1. Takahashi, K. *et al.* Induction of pluripotent stem cells from adult human fibroblasts by defined factors. *cell* **131**, 861-872 (2007).
2. Hattori, N. Cerebral organoids model human brain development and microcephaly. *Movement Disorders* **2**, 185-185 (2014).
3. Lancaster, M.A. & Knoblich, J.A. Generation of cerebral organoids from human pluripotent stem cells. *Nature protocols* **9**, 2329-2340 (2014).
4. Lancaster, M.A. & Huch, M. Disease modelling in human organoids. *Disease models & mechanisms* **12**, dmm039347 (2019).
5. Kim, J., Koo, B.-K. & Knoblich, J.A. Human organoids: model systems for human biology and medicine. *Nature Reviews Molecular Cell Biology* **21**, 571-584 (2020).
6. Logan, S. *et al.* Studying human neurological disorders using induced pluripotent stem cells: from 2D monolayer to 3D organoid and blood brain barrier models. *Comprehensive Physiology* **9**, 565-611 (2011).
7. Chen, H.I., Song, H. & Ming, G.l. Applications of human brain organoids to clinical problems. *Developmental Dynamics* **248**, 53-64 (2019).
8. Qian, X., Song, H. & Ming, G.-l. Brain organoids: advances, applications and challenges. *Development* **146** (2019).
9. Marx, V. Reality check for organoids in neuroscience. *Nature Methods* **17**, 961-964 (2020).
10. Workman, M.J. & Svendsen, C.N. Recent advances in human iPSC-derived models of the blood–brain barrier. *Fluids and Barriers of the CNS* **17**, 1-10 (2020).
11. Zhao, Z., Nelson, A.R., Betsholtz, C. & Zlokovic, B.V. Establishment and dysfunction of the blood-brain barrier. *Cell* **163**, 1064-1078 (2015).
12. Wang, H. Modeling neurological diseases with human brain organoids. *Frontiers in synaptic neuroscience* **10**, 15 (2018).
13. Chen, A., Guo, Z., Fang, L. & Bian, S. Application of Fused Organoid Models to Study Human Brain Development and Neural Disorders. *Frontiers in Cellular Neuroscience* (2020).
14. Qian, X. *et al.* Generation of human brain region–specific organoids using a miniaturized spinning bioreactor. *Nature protocols* **13**, 565 (2018).
15. Bhaduri, A. *et al.* Cell stress in cortical organoids impairs molecular subtype specification. *Nature* **578**, 142-148 (2020).

16. Association, A.s. 2019 Alzheimer's disease facts and figures. *Alzheimer's & Dementia* **15**, 321-387 (2019).
17. 2020 Alzheimer's disease facts and figures. *Alzheimer's & Dementia* **16**, 391-460 (2020).
18. De Strooper, B. & Karran, E. The cellular phase of Alzheimer's disease. *Cell* **164**, 603-615 (2016).
19. Esmail, S. & Danter, W.R. DeepNEU: artificially induced stem cell (aiPSC) and differentiated skeletal muscle cell (aiSkMC) simulations of infantile onset POMPE disease (IOPD) for potential biomarker identification and drug discovery. *Frontiers in cell and developmental biology* **7**, 325 (2019).
20. Danter, W.R. DeepNEU: cellular reprogramming comes of age–a machine learning platform with application to rare diseases research. *Orphanet Journal of Rare Diseases* **14**, 13 (2019).
21. Esmail, S. & Danter, W.R. Viral pandemic preparedness: A pluripotent stem cell-based machine-learning platform for simulating SARS-CoV-2 infection to enable drug discovery and repurposing. *Stem cells translational medicine* (2020).
22. Santos, C.R., Cardoso, I. & Gonçalves, I. Key enzymes and proteins in amyloid-β production and clearance. *Alzheimer's Disease Pathogenesis—Core Concepts, Shifting Paradigms and Therapeutic Targets; de la Monte, S., Ed*, 53-86 (2011).
23. Lippmann, E.S. *et al.* Deterministic HOX patterning in human pluripotent stem cell-derived neuroectoderm. *Stem cell reports* **4**, 632-644 (2015).
24. Ahn, J.-I. *et al.* Comprehensive transcriptome analysis of differentiation of embryonic stem cells into midbrain and hindbrain neurons. *Developmental biology* **265**, 491-501 (2004).
25. Kirsch, L., Liscovitch, N. & Chechik, G. Localizing genes to cerebellar layers by classifying ISH images. *PLoS Comput Biol* **8**, e1002790 (2012).
26. Logan, S. *et al.* Dynamic Characterization of Structural, Molecular, and Electrophysiological Phenotypes of Human-Induced Pluripotent Stem Cell-Derived Cerebral Organoids, and Comparison with Fetal and Adult Gene Profiles. *Cells* **9**, 1301 (2020).
27. Papaspyropoulos, A., Tsolaki, M., Foroglou, N. & Pantazaki, A.A. Modeling and Targeting Alzheimer's Disease With Organoids. *Frontiers in Pharmacology* **11**, 396 (2020).
28. Kim, H. *et al.* Pluripotent stem cell-derived cerebral organoids reveal human oligodendrogenesis with dorsal and ventral origins. *Stem cell reports* **12**, 890-905 (2019).
29. Gerakis, Y. & Hetz, C. Brain organoids: a next step for humanized Alzheimer's disease models? *Molecular Psychiatry* **24**, 474-478 (2019).
30. Espuny-Camacho, I. *et al.* Human pluripotent stem-cell-derived cortical neurons integrate functionally into the lesioned adult murine visual cortex in an area-specific way. *Cell reports* **23**, 2732-2743 (2018).
31. Zemke, M. *et al.* Loss of Ezh2 promotes a midbrain-to-forebrain identity switch by direct gene derepression and Wnt-dependent regulation. *BMC biology* **13**, 1-14 (2015).
32. Krefft, O., Jabali, A., Iefremova, V., Koch, P. & Ladewig, J. Generation of standardized and reproducible forebrain-type cerebral organoids from human induced pluripotent stem cells. *JoVE (Journal of*

Visualized Experiments), e56768 (2018).

33. Do, J.T. & Hong, Y.J. Neural lineage differentiation from pluripotent stem cells to mimic human brain tissues. *Frontiers in Bioengineering and Biotechnology* **7**, 400 (2019).
34. Tkachenko, L.A., Zykin, P.A., Nasyrov, R.A. & Krasnoshchekova, E.I. Distinctive features of the human marginal zone and Cajal–Retzius cells: comparison of morphological and immunocytochemical features at midgestation. *Frontiers in neuroanatomy* **10**, 26 (2016).
35. Velasco, S. *et al.* Individual brain organoids reproducibly form cell diversity of the human cerebral cortex. *Nature* **570**, 523-527 (2019).
36. McKenzie, A.T. *et al.* Brain cell type specific gene expression and co-expression network architectures. *Scientific reports* **8**, 1-19 (2018).
37. Romito-DiGiacomo, R.R., Menegay, H., Cicero, S.A. & Herrup, K. Effects of Alzheimer's disease on different cortical layers: the role of intrinsic differences in Aβ susceptibility. *Journal of Neuroscience* **27**, 8496-8504 (2007).
38. Madadi, S., Schwarzenbach, H., Saidijam, M., Mahjub, R. & Soleimani, M. Potential microRNA-related targets in clearance pathways of amyloid-β: novel therapeutic approach for the treatment of Alzheimer's disease. *Cell & bioscience* **9**, 91 (2019).
39. Arbor Ph D, S. Targeting amyloid precursor protein shuttling and processing-long before amyloid beta formation. *Neural Regeneration Research* **12**, 207 (2017).
40. Raja, W.K. *et al.* Self-organizing 3D human neural tissue derived from induced pluripotent stem cells recapitulate Alzheimer's disease phenotypes. *PloS one* **11**, e0161969 (2016).
41. Brighi, C., Cordella, F., Chiriatti, L., Soloperto, A. & Di Angelantonio, S. Retinal and Brain Organoids: Bridging the Gap Between in vivo Physiology and in vitro Micro-Physiology for the Study of Alzheimer's Diseases. *Frontiers in Neuroscience* **14** (2020).
42. Silva, T.P. *et al.* Maturation of human pluripotent stem cell-derived cerebellar neurons in the absence of co-culture. *Frontiers in Bioengineering and Biotechnology* **8**, 70 (2020).
43. Ribeiro, M.M., Okawa, S. & Del Sol, A. (Wiley Online Library, 2020).
44. Addinsoft (Addinsoft Long Island, New York, 2019).
45. Groumpos, P.P. Deep learning vs. wise learning: a critical and challenging overview. *IFAC-PapersOnLine* **49**, 180-189 (2016).

Figures

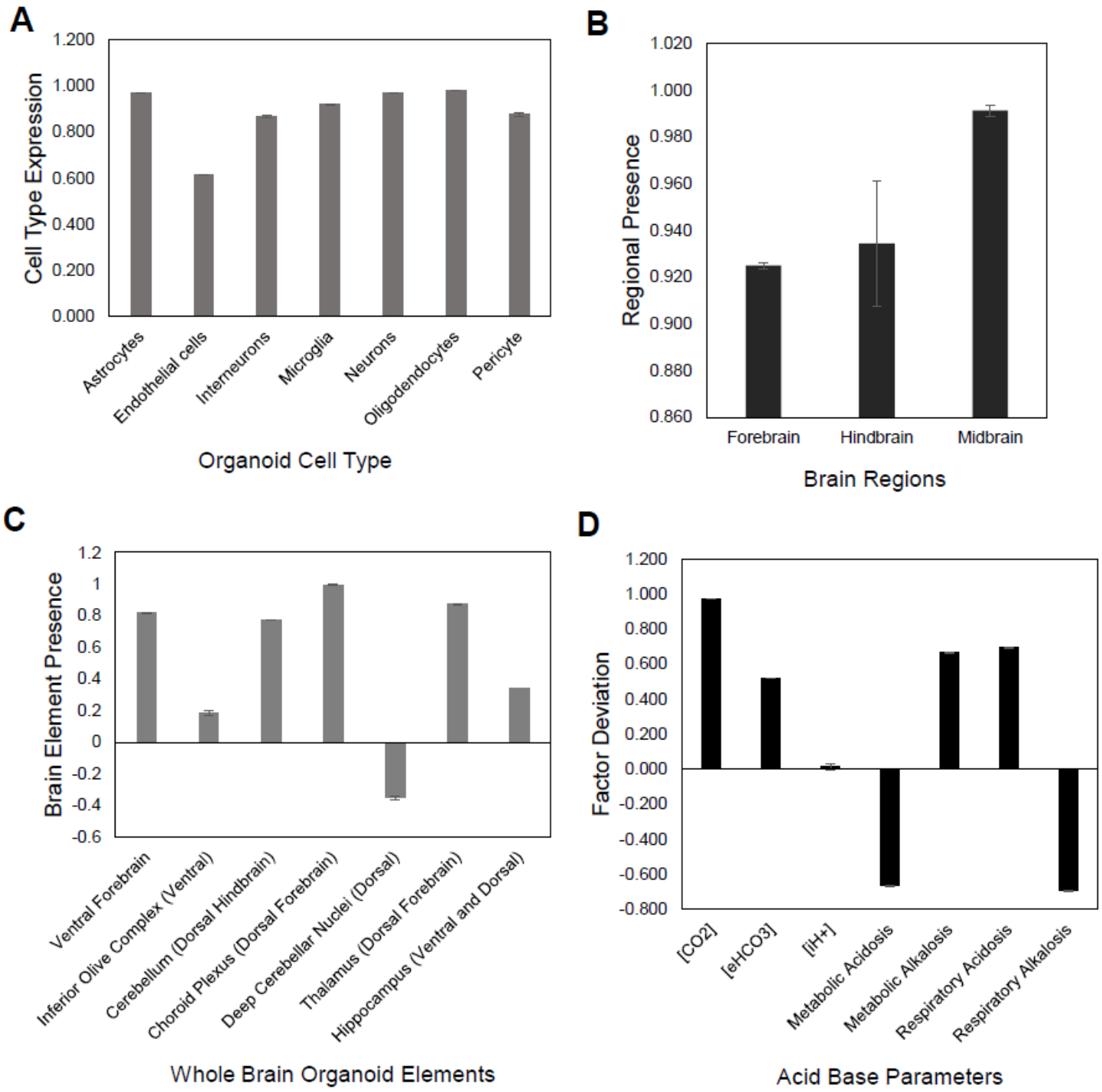

Figure 1

DeepNEU simulation of differentiated WT aiWBO cell types, regions, elements and acid base status. A, Expression of basic aiWBO cell types based on genotypic markers. B, Presence of the three aiWBO brain regions based on genotypic markers. C, Presence of the ventral and dorsal aiWBO brain elements based on genotypic markers. D, The acid base status of the aiWBO based on phenotypic factors. The vertical y-axes represent the semiquantitative levels of concepts that are estimated by DeepNEU regarding an arbitrary base line where 0 = base line, 1 = maximum expression or presence and -1 = minimal expression

level or presence. The horizontal x-axes represent the individual aiWBO concepts being simulated. Data represent mean of three experiments ± 95% confidence interval.

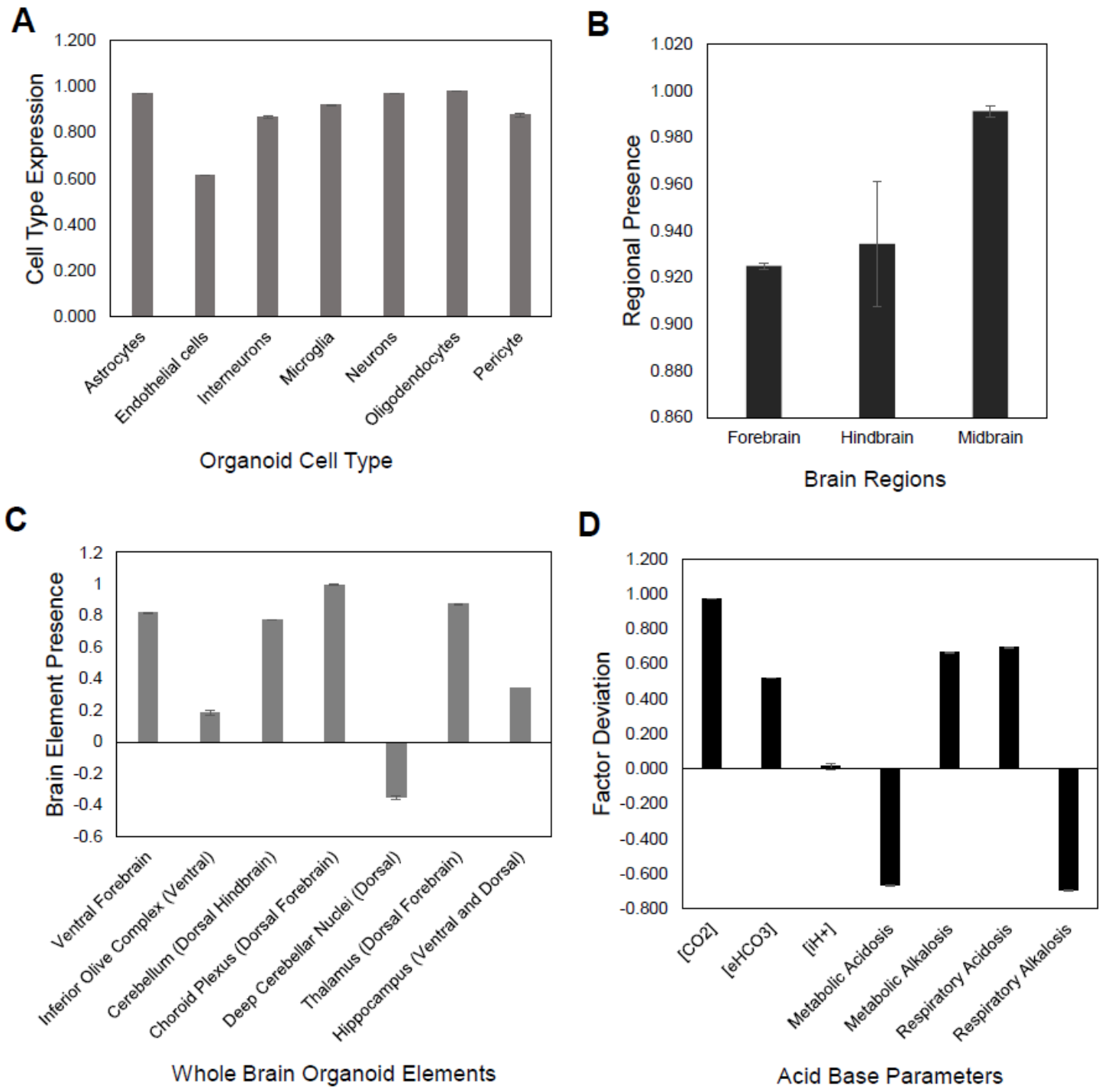

Figure 1

DeepNEU simulation of differentiated WT aiWBO cell types, regions, elements and acid base status. A, Expression of basic aiWBO cell types based on genotypic markers. B, Presence of the three aiWBO brain regions based on genotypic markers. C, Presence of the ventral and dorsal aiWBO brain elements based on genotypic markers. D, The acid base status of the aiWBO based on phenotypic factors. The vertical y-axes represent the semiquantitative levels of concepts that are estimated by DeepNEU regarding an

arbitrary base line where 0 = base line, 1 = maximum expression or presence and -1 = minimal expression level or presence. The horizontal x-axes represent the individual aiWBO concepts being simulated. Data represent mean of three experiments ± 95% confidence interval.

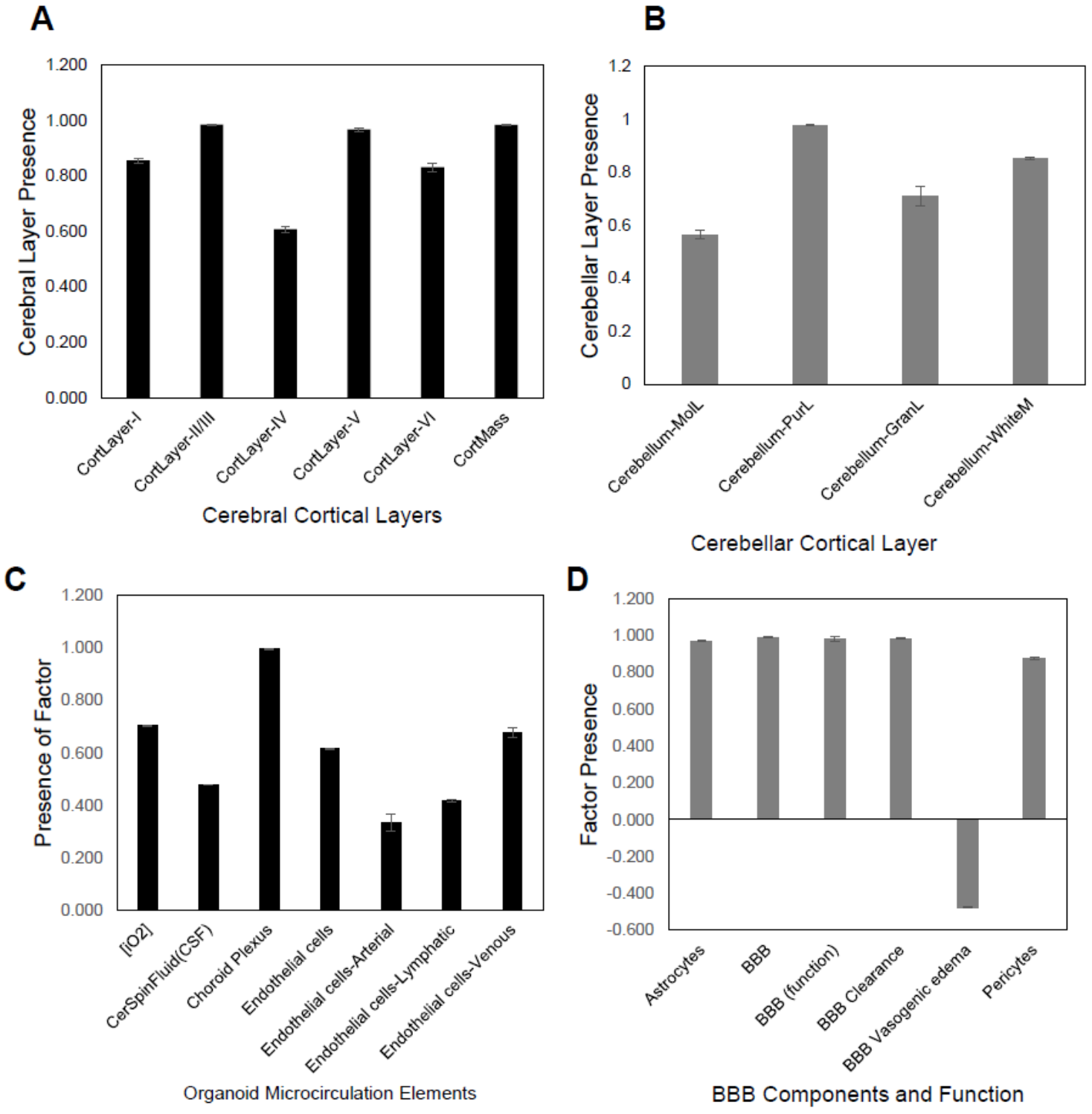

Figure 2

DeepNEU simulation of cerebral cortical layers, cerebellar cortical layers, microcirculation and BBB of WT aiWBO. A, Presence of the six aiWBO cerebral cortical layers based on genotypic markers. An estimate of cortical mass is derived by combining the six cortical layers. B, Presence of the four cerebellar layers

based on genotypic markers. C, Presence of aiWBO microcirculation elements based on phenotypic markers. D, The presence of aiWBO BBB elements and function based on phenotypic factors. The vertical y-axes represent the semiquantitative levels of concepts that are estimated by DeepNEU regarding an arbitrary base line where 0 = base line, 1 = maximum expression or presence and -1 = minimal expression level or presence. The horizontal x-axes represent the individual aiWBO concepts being simulated. Data represent mean of three experiments ± 95% confidence interval.

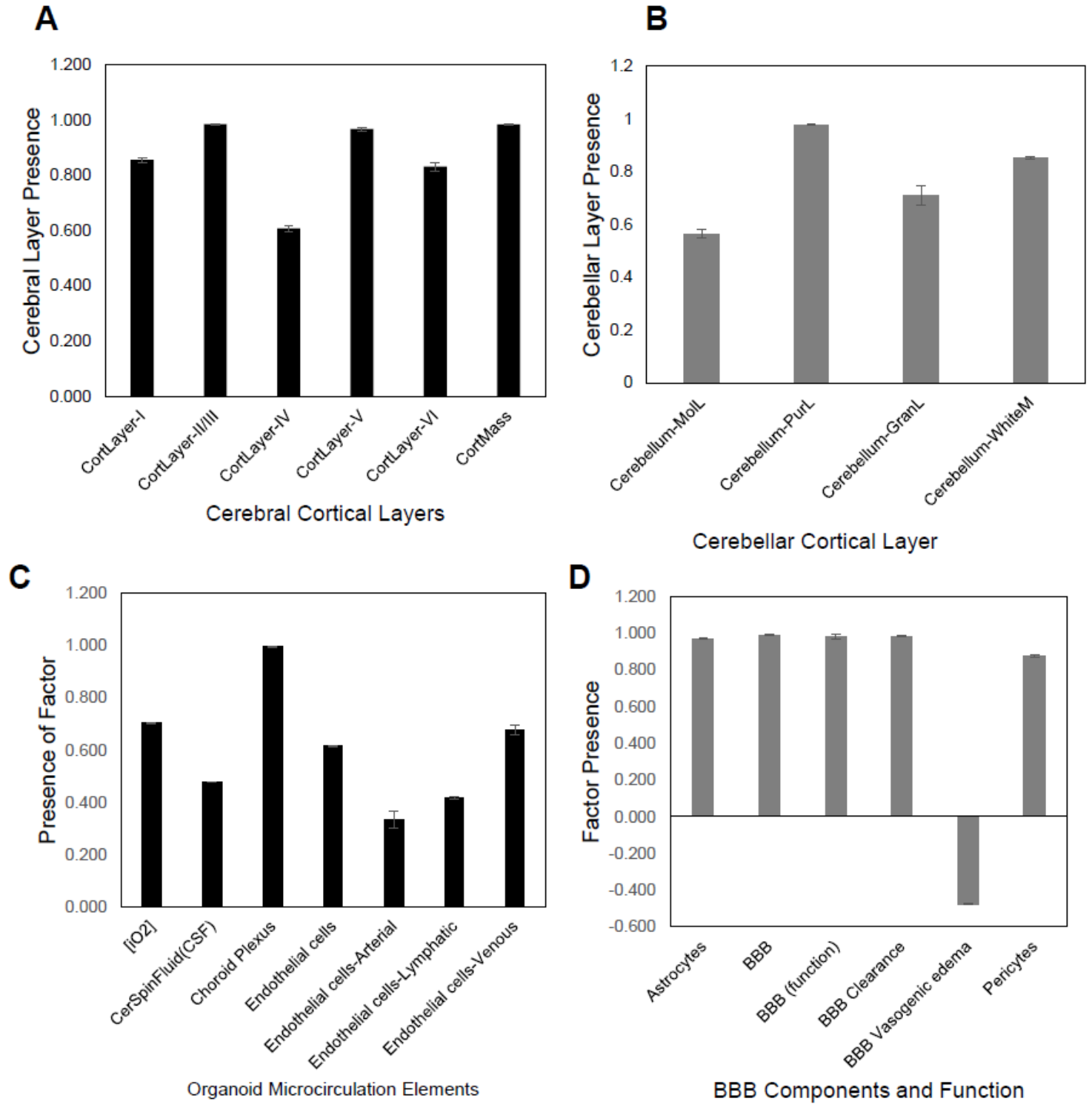

Figure 2

DeepNEU simulation of cerebral cortical layers, cerebellar cortical layers, microcirculation and BBB of WT aiWBO. A, Presence of the six aiWBO cerebral cortical layers based on genotypic markers. An estimate of cortical mass is derived by combining the six cortical layers. B, Presence of the four cerebellar layers based on genotypic markers. C, Presence of aiWBO microcirculation elements based on phenotypic markers. D, The presence of aiWBO BBB elements and function based on phenotypic factors. The vertical y-axes represent the semiquantitative levels of concepts that are estimated by DeepNEU regarding an arbitrary base line where 0 = base line, 1 = maximum expression or presence and -1 = minimal expression level or presence. The horizontal x-axes represent the individual aiWBO concepts being simulated. Data represent mean of three experiments ± 95% confidence interval.

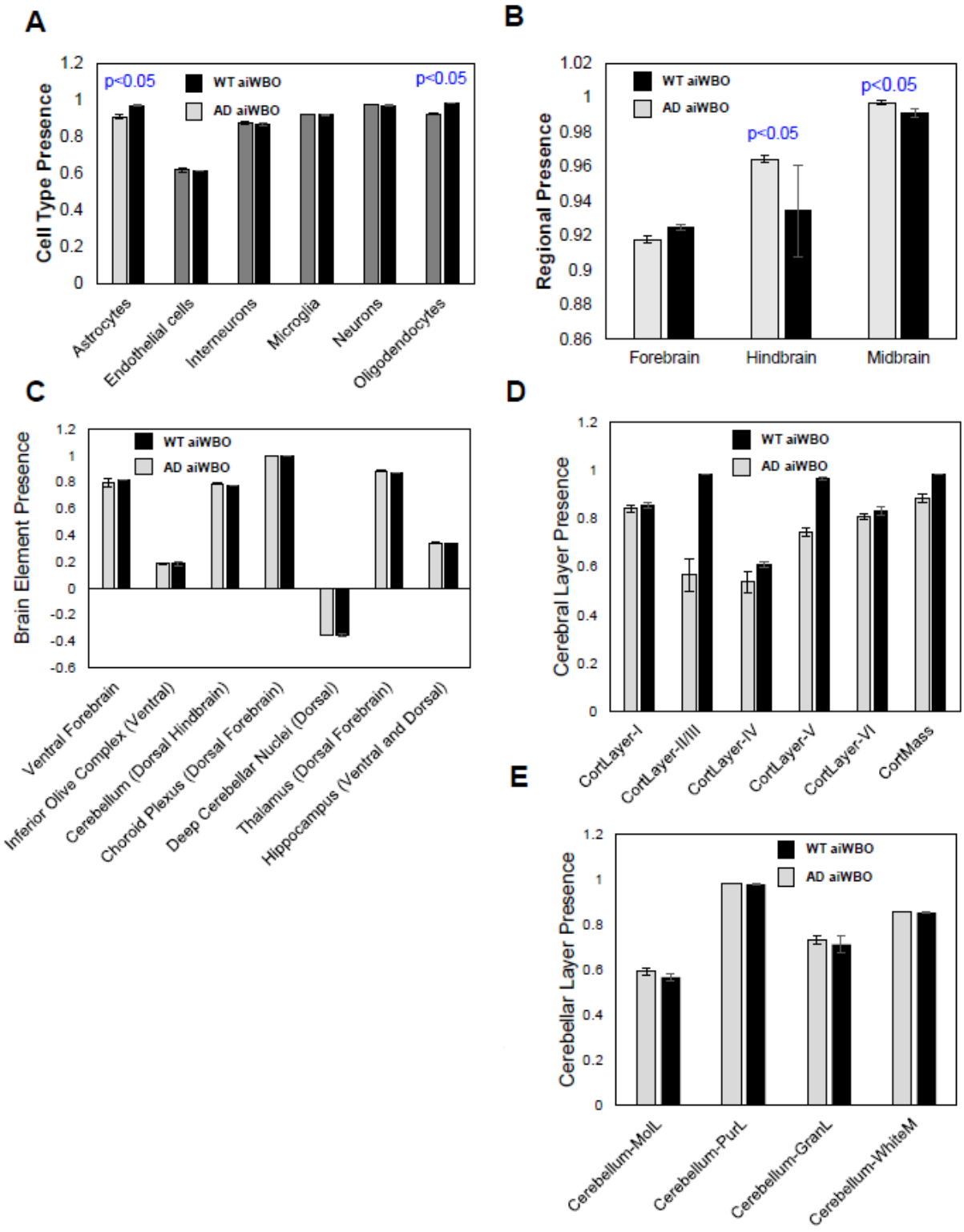

Figure 3

Comparison of aiWBO-WT vs aiWBO-AD simulation results. A, Comparison of aiWBO simulations of WT vs AD cell types. B, Comparison of brain region concepts in WT vs AD simulations, C, Comparison of ventral-dorsal concepts in WT vs AD simulations. D, Comparison of cerebral cortical layers in WT vs AD simulations. E, Comparison of cerebellar cortical layers in WT and AD simulations. The vertical y-axes represent the semiquantitative levels of concepts that are estimated by DeepNEU regarding an arbitrary

base line where 0 = base line, 1 = maximum expression or presence and -1 = minimal expression level or presence. The horizontal x-axes represent the individual aiWBO concepts being simulated. Data represent mean of three experiments ± 95%confidence interval. All p-values from Mann-Whitney u test.

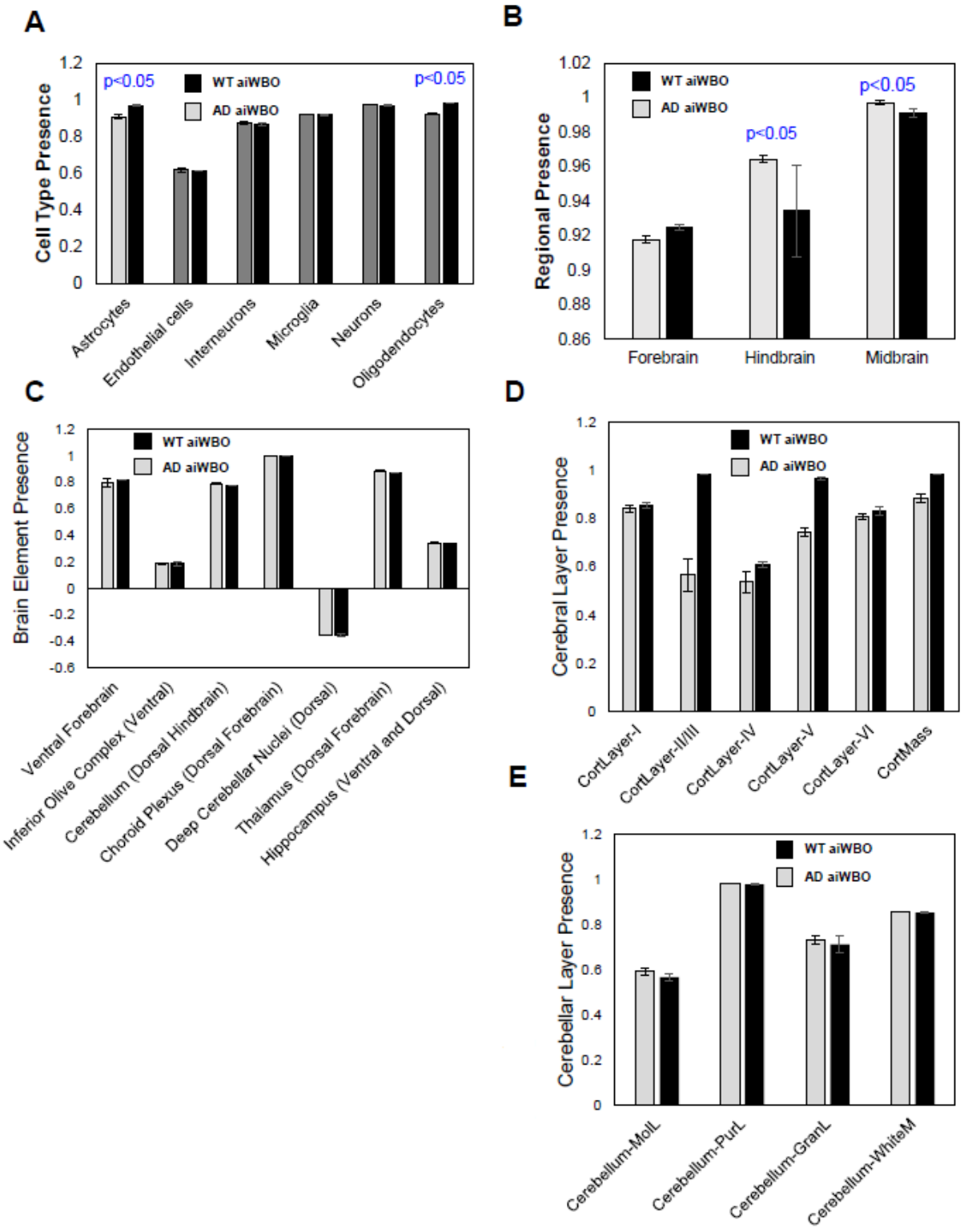

Figure 3

Comparison of aiWBO-WT vs aiWBO-AD simulation results. A, Comparison of aiWBO simulations of WT vs AD cell types. B, Comparison of brain region concepts in WT vs AD simulations, C, Comparison of

ventral-dorsal concepts in WT vs AD simulations. D, Comparison of cerebral cortical layers in WT vs AD simulations. E, Comparison of cerebellar cortical layers in WT and AD simulations. The vertical y-axes represent the semiquantitative levels of concepts that are estimated by DeepNEU regarding an arbitrary base line where 0 = base line, 1 = maximum expression or presence and -1 = minimal expression level or presence. The horizontal x-axes represent the individual aiWBO concepts being simulated. Data represent mean of three experiments ± 95%confidence interval. All p-values from Mann-Whitney u test.

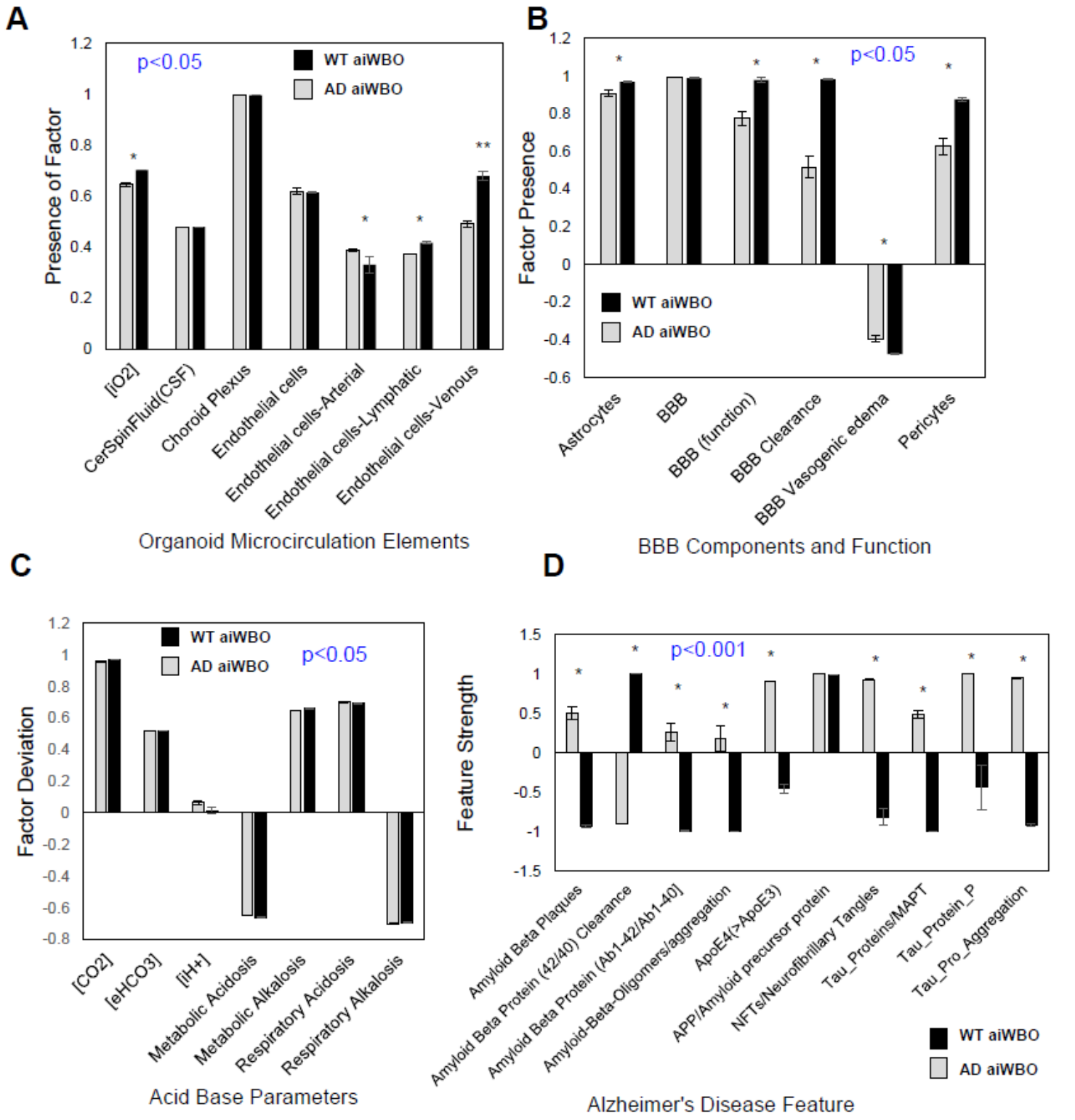

Figure 4

Comparison of aiWBO-WT vs aiWBO-AD simulation results for microcirculation, BBB, Acid-Base status and Alzheimer's Disease (AD) features. A, Comparison of microcirculation elements in WT vs AD simulations, B, Comparison of BBB concepts in WT vs AD simulations, C, Comparison of acid base concepts in WT vs AD simulations. D, Comparison of Alzheimer's Disease features in WT vs AD simulations. The vertical y-axes represent the semiquantitative levels of concepts that are estimated by DeepNEU regarding an arbitrary base line where 0 = base line, 1 = maximum expression or presence and -1 = minimal expression level or presence. The horizontal x-axes represent the individual aiWBO concepts being simulated. Data represent mean of three experiments ± 95% confidence interval. All p values from Mann-Whitney u test.

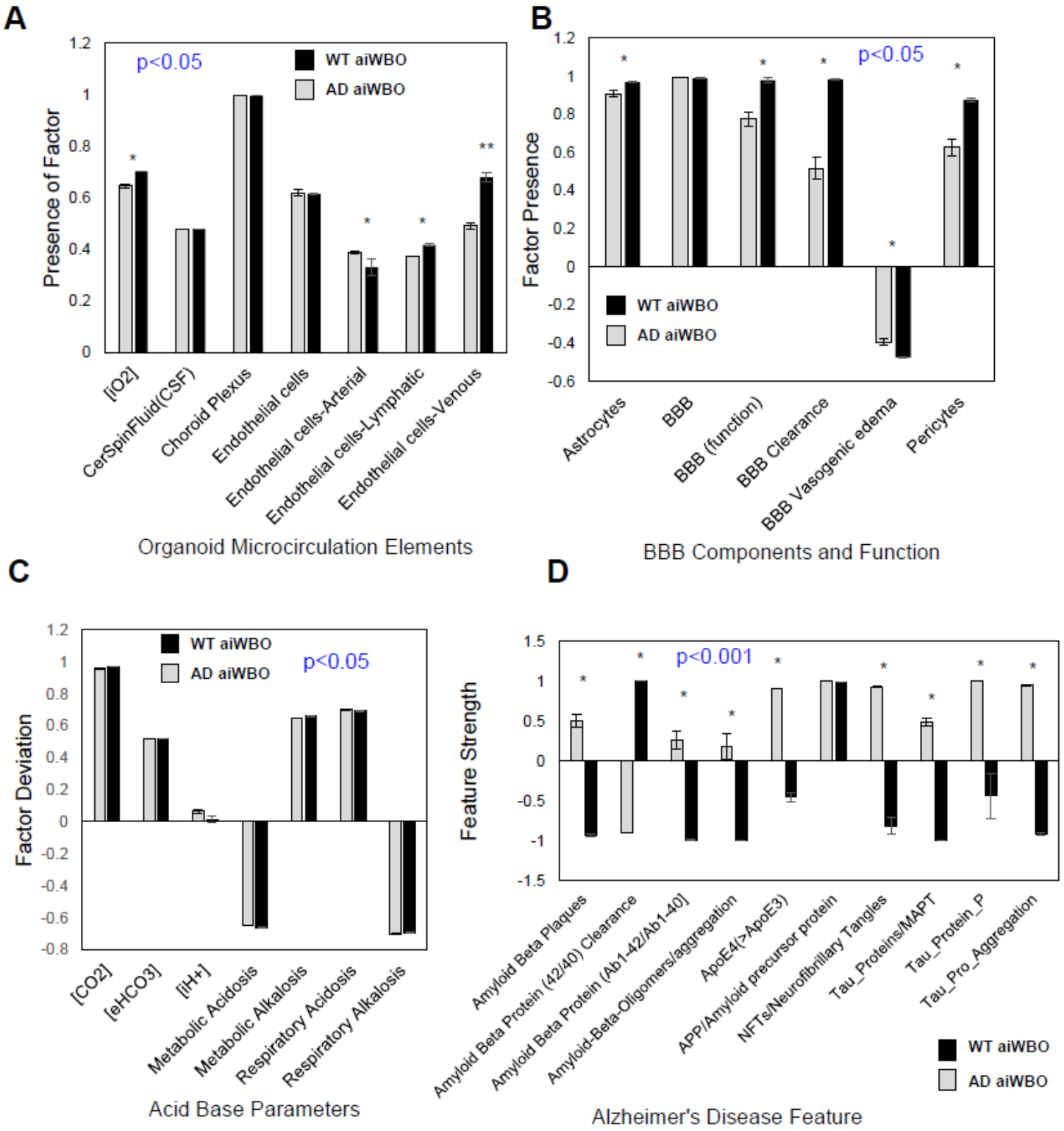

Figure 4

Comparison of aiWBO-WT vs aiWBO-AD simulation results for microcirculation, BBB, Acid-Base status and Alzheimer's Disease (AD) features. A, Comparison of microcirculation elements in WT vs AD simulations, B, Comparison of BBB concepts in WT vs AD simulations, C, Comparison of acid base concepts in WT vs AD simulations. D, Comparison of Alzheimer's Disease features in WT vs AD simulations. The vertical y-axes represent the semiquantitative levels of concepts that are estimated by

DeepNEU regarding an arbitrary base line where 0 = base line, 1 = maximum expression or presence and -1 = minimal expression level or presence. The horizontal x-axes represent the individual aiWBO concepts being simulated. Data represent mean of three experiments ± 95% confidence interval. All p values from Mann-Whitney u test.

Supplementary Files

This is a list of supplementary files associated with this preprint. Click to download.

- EsmailandDanterSupplmentaryinformationFinal.docx
- EsmailandDanterSupplmentaryinformationFinal.docx